

Temperature and wavelength dependence of Fermi-tail photoemission and two-photon photoemission from multialkali semiconductors

Mark C. Booth,^{a)} Bahaa E. A. Saleh, Alexander V. Sergienko, and Malvin C. Teich^{b)}
*Quantum Imaging Laboratory,^{c)} Department of Electrical and Computer Engineering, Boston University,
 8 Saint Mary's Street, Boston, Massachusetts 02215; Department of Physics, Boston University,
 590 Commonwealth Avenue, Boston, Massachusetts 02215; and Biomedical Engineering, Boston University,
 44 Cummings Street, Boston, Massachusetts 02215*

(Received 24 June 2005; accepted 26 May 2006; published online 25 July 2006)

Two-photon photoemission is a useful technique for examining interface, surface, and image-potential states in various materials. We report the temperature and wavelength dependences of the two-photon photoemission yield for several multialkali semiconductors used as photocathode materials in commercially available photomultiplier tubes. We also report the dependence on temperature and wavelength of one-photon photoemission associated with the Fermi tail of the electron-occupancy probability distribution, which can mask two-photon photoemission. The results are expected to be of use in entangled-photon photoemission experiments, for which a large value of the two-photon photoemission yield is required. © 2006 American Institute of Physics.

[DOI: 10.1063/1.2218037]

I. INTRODUCTION

In principle, ordinary (one-photon) photoemission cannot occur when the energy of a single incident photon is inadequate to effect the release of an electron from the valence band of a semiconductor into the vacuum.¹ However, two photons can team up and result in a process known as two-photon photoemission.^{2,3} This process involves the near simultaneous absorption of a pair of photons whose sum energy, $2h\nu$, is sufficient to cause the electron to escape to the vacuum.⁴ As depicted in Fig. 1 at $T=0$ K, this requires that $2h\nu > E_g + \chi$, where h is Planck's constant, ν is the optical frequency of the incident light, E_g is the band gap energy, and χ is the electron affinity.⁵

At finite temperatures ($T > 0$ K), the Fermi-Dirac electron-occupation distribution in the semiconductor dictates that some electrons, known as "Fermi-tail electrons," possess sufficient thermal excitation to reside in the conduction band, with the preponderance of them at the bottom thereof.⁵ Under those conditions, as is evident from the sketch in Fig. 1, a single photon can release an electron into the vacuum. The result is Fermi-tail (one-photon) photoemission⁶ which, in general, coexists with two-photon photoemission. Fermi-tail photoemission often serves as a pesky masker of two-photon photoemission. The physical origin of this process makes it clear that the magnitude of the Fermi-tail photocurrent will depend on sample temperature as well as on the photon energy (wavelength) of the illumination. This expectation is borne out by the results presented in Sec. IV: as expected, the one-photon photocurrent increases with increasing temperature (since the number of electrons available in the Fermi tail increases with tempera-

ture) and with increasing photon energy (since the probability of occupancy is greater toward the bottom of the conduction band).

On the other hand, the underlying process involved in two-photon photoemission leads us to expect that the two-photon photocurrent will be relatively independent of material temperature, provided that twice the absorbed photon energy is sufficiently greater than the photoelectric threshold. This expectation, too, is experimentally borne out, as reported in Sec. III. The relative strength of the two-photon photoemission effect is provided in Sec. V for various multi-alkali semiconductors.

II. THEORY

Experiments designed to observe two-photon photoemission generally return a photocurrent i that comprises three contributions: (1) detection-system and circuit noise, which produces a constant background current that is roughly i_{ckt}

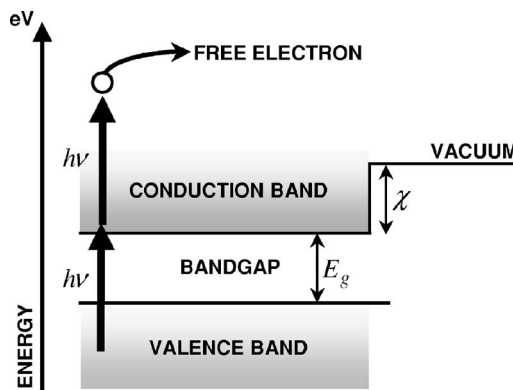


FIG. 1. Idealized band structure for a semiconductor material such as K_2CsSb with electron affinity χ and band gap energy E_g . The maximum kinetic energy imparted to a photoelectron by a pair of photons, each of energy $h\nu$, is $E_{\text{max}} = 2h\nu - (E_g + \chi)$. A single photon can release a "Fermi-tail" electron into the vacuum.

^{a)}Present address: Georgia Institute of Technology, Department of Biomedical Engineering, 313 Ferst Drive, Atlanta, GA 30332-0535.

^{b)}Electronic mail: teich@bu.edu

^{c)}Quantum Imaging Laboratory homepage: <http://www.bu.edu/qil>

$\sim 10^{-18}$ A in our experiments; (2) one-photon photoemission from thermally excited electrons in the Fermi tail, which leads to a photocurrent proportional to the optical power;⁶ and (3) two-photon photoemission arising from the absorption of pairs of photons, which leads to a photocurrent proportional to the square of the optical power and inversely proportional to the illumination area \mathcal{A} .⁷

For a continuous wave (cw) optical beam and a lossless optical system, the overall photocurrent $i(\lambda, T)$ is then expressed as⁸

$$i(\lambda, T) = i_{\text{ckt}} + Y_F(\lambda, T)P_0 + L(\lambda, T)P_0^2/\mathcal{A} \quad (1)$$

$$= i_{\text{ckt}} + Y_F(\lambda, T)P_0 + L(\lambda, T)I_0P_0 \quad (2)$$

$$= i_{\text{ckt}} + Y_F(\lambda, T)P_0 + \Lambda(\lambda, T)P_0, \quad (3)$$

where the first, second, and third terms on the right-hand sides of the equations are, respectively, the three contributions indicated above. The parameter P_0 is the optical power, λ represents the wavelength of the incident radiation, and T is the temperature of the material. The quantity $Y_F(\lambda, T)$ is the one-photon Fermi-tail photoemission yield (units of A/W).⁶ The two-photon photoemission yield $\Lambda(\lambda, T) = L(\lambda, T)I_0$, which serves as a measure of the strength of two-photon photoemission, also has units of A/W.⁷ By virtue of the fact that two-photon photoemission is a second-order process,^{8,9} $\Lambda(\lambda, T)$ contains an intrinsic proportionality to the incident light intensity I_0 (units of W/cm²), which accommodates the inverse area dependence indicated in Eq. (1). In contrast, the one-photon Fermi-tail photoemission yield $Y_F(\lambda, T)$ depends only on the optical power P_0 and not on the intensity of the illumination.

The idealized results presented in Eqs. (1)–(3) must be modified in the presence of any of the following features: (1) optical loss in the system, which reduces the optical power incident on the sample; (2) the use of a light chopper in conjunction with phase-sensitive detection, which introduces optical power loss and also results in only the first harmonic of the induced photocurrent being extracted; and (3) the use of a pulsed optical source, which results in an increase of the two-photon photocurrent relative to that for a cw source of the same mean power by virtue of the square-law power dependence of the process.

In this case, Eqs. (1)–(3) are rewritten as

$$i(\lambda, T) = i_{\text{ckt}} + \mathcal{F}_1[Y_F(\lambda, T)(\mathcal{T}P_0) + L(\lambda, T)(\mathcal{T}P_0)^2\Gamma/\mathcal{A}] \quad (4)$$

$$= i_{\text{ckt}} + \mathcal{F}_1[Y_F(\lambda, T)(\mathcal{T}P_0) + L(\lambda, T)(\mathcal{T}I_0)(\mathcal{T}P_0)\Gamma] \quad (5)$$

$$= i_{\text{ckt}} + \mathcal{F}_1[Y_F(\lambda, T)(\mathcal{T}P_0) + \Lambda(\lambda, T)(\mathcal{T}P_0)\Gamma], \quad (6)$$

where \mathcal{T} represents the fraction of the light power that actually reaches the sample under study; this transmittance accommodates absorption and reflection losses in the optical system as well as reflection at the sample.^{8,10} The quantity \mathcal{F}_1 represents the first Fourier component of the modulated square-wave wave form resulting from the transmission of the illumination through the light chopper; only the first Fourier component is extracted in a phase-sensitive detection scheme.^{7,8}

The factor Γ in these equations accounts for the fact that a pulsed optical source served as the source of illumination in our experiments; the output of the mode-locked laser comprises a sequence of brief optical pulses. Since the two-photon photocurrent is proportional to the square of the incident optical power, as indicated in Eq. (4), a sequence of brief but powerful optical pulses is more effective for eliciting two-photon photoemission than is a cw optical beam of the same mean power. Stated differently, two-photon photoemission is induced by the mean-square optical power and not by the square-mean optical power. The expression for the two-photon photocurrent may be expressed in terms of the latter by incorporating a factor Γ in Eqs. (4)–(6) such that

$$\Gamma \equiv \frac{1}{\tau_1} \int_0^{\tau_1} P^2(t) dt \bigg/ \left[\frac{1}{\tau_1} \int_0^{\tau_1} P(t) dt \right]^2. \quad (7)$$

This quantity represents the ratio of the mean-square of the light-power wave form, to its square-mean, over a time τ_1 that is conveniently taken to be one period of the mode-locked laser output.

It is convenient to express Γ in terms of the duty cycle of the mode-locked laser output. Let us assume, for simplicity, that the optical pulses are rectangular, of duration τ_0 , and separated from each other by the interval τ_1 . We readily compute the peak power P of a single mode-locked pulse that is equivalent to a cw beam of mean power P_0 ,

$$P\tau_0 = P_0\tau_1, \quad (8)$$

so that

$$P = P_0(\tau_1/\tau_0) = P_0/\Delta, \quad (9)$$

where Δ is defined as the duty cycle of the mode-locked laser output,

$$\Delta \equiv \tau_0/\tau_1. \quad (10)$$

Thus, the mean-square power is

$$\frac{1}{\tau_1} \int_0^{\tau_0} \left(\frac{P_0}{\Delta} \right)^2 dt = \frac{1}{\tau_1} \left(\frac{P_0}{\Delta} \right)^2 \tau_0 = \frac{P_0^2}{\Delta}, \quad (11)$$

whereas the square-mean power is P_0^2 . We conclude that the enhancement factor Γ specified in Eq. (7) is approximately given by

$$\Gamma = (P_0^2/\Delta)/P_0^2 = 1/\Delta. \quad (12)$$

The one-photon Fermi-tail photocurrent, in contrast, depends only on the mean optical power P_0 presented to the sample and not on any feature of its temporal variation. It is, however, affected by the factors \mathcal{T} and \mathcal{F}_1 since these quantities are associated with optical loss and phase-sensitive detection.

III. TEMPERATURE AND WAVELENGTH DEPENDENCE OF TWO-PHOTON PHOTOEMISSION

We carried out a series of two-photon photoemission experiments from multialkali semiconductors at various temperatures and wavelengths using the experimental configuration shown in Fig. 2. A photomultiplier-tube (PMT)

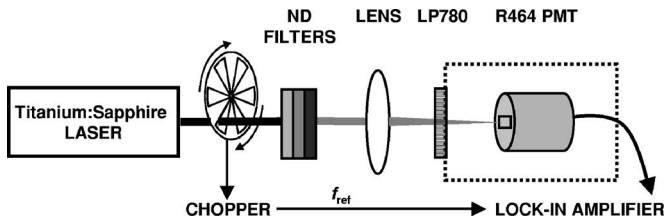


FIG. 2. Experimental arrangement for two-photon photoemission. The pulsed output of a titanium:sapphire laser operated at wavelength λ is focused by a lens of focal length $f=88$ mm onto the multialkali-semiconductor photocathode of a photomultiplier tube (PMT) operated at temperature T . The PMT signal is directed to a lock-in amplifier that is referenced to the frequency $f_{\text{ref}}=150$ Hz of a rotating optical chopper. Neutral density (ND) filters are used to attenuate the laser power and a long-pass optical filter (LP 780) isolates the detector from stray room light.

configuration, in which the semiconductor material under consideration comprises the photocathode, was purposely used to take advantage of the near noise-free current gain available in such devices.⁸

A titanium:sapphire laser (Tsunami, Spectra-Physics, Mountain View, CA) was operated at a wavelength of $\lambda=800$ nm ($h\nu=1.55$ eV), 830 nm ($h\nu=1.50$ eV), or 845 nm ($h\nu=1.47$ eV). The mode-locked output consisted of a sequence of 120 fs duration light pulses of approximately Gaussian shape, emitted at a rate of 82 MHz. Approximating the light pulses as square, the duty cycle [see Eq. (10)] is then calculated to be $\Delta \equiv \tau_0/\tau_1=(120 \times 10^{-15})(82 \times 10^6) \approx 10^{-5}$. The laser light was fed through a mechanical chopper operated at a reference frequency of 150 Hz, which further reduced the duty cycle by a factor of 2; Eq. (12) therefore provides $\Gamma=1/(\Delta/2) \approx 2 \times 10^5$.

A lens of focal length $f=88$ mm focused the light into a small spot on the multialkali-semiconductor photocathode of the photomultiplier tube. This dramatically increases the value of \mathcal{I}_0 , and thence the two-photon photocurrent in Eq. (5). In the experiments reported in this section, the illuminated area of the photocathode was maintained at $\approx 2.5 \times 10^{-5}$ cm², as estimated by the properties of the focusing lens. A long-pass filter (LP 780) served to isolate the detector from stray room light.

The mean laser output power P_0 incident on the faceplate of the photomultiplier tube was measured with a model 818-SL laser power meter (Newport Corp., Irvine, CA) placed directly in front of the faceplate of the PMT. The maximum mean laser power never exceeded 20 μ W to eliminate the possibility of local heating effects. The focused laser pulses did not result in a temperature increase at the photocathode as was verified by observing the stability of the mean photocurrent and its standard deviation over a 3 min acquisition period. Calibrated neutral-density (ND) filters (Wratten, Eastman Kodak, Rochester, NY) were used to attenuate the laser power for a sequence of measurements. Thin Wratten ND filters were purposely chosen to minimize changes in the area of the focused spot on filter insertion. The output of the PMT was fed to a lock-in amplifier (Stanford Research Systems 850, Sunnyvale, CA), for which the light-chopper provided the reference signal.

The temperature dependence of the two-photon photocurrent from a K_2CsSb multialkali semiconductor photocath-

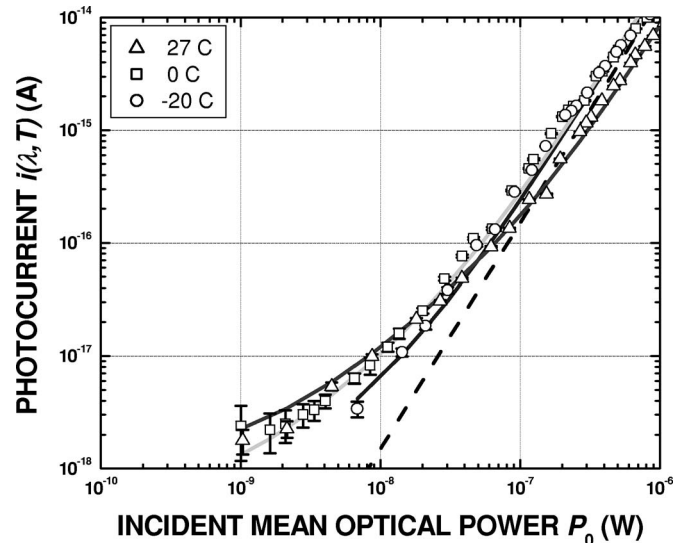


FIG. 3. Two-photon photoemission from a K_2CsSb -semiconductor photocathode in a Hamamatsu R464 PMT. The double-logarithmic plot displays the fundamental component of the photoelectric current at the cathode (amperes) vs the mean optical power (watts) incident on the faceplate of the PMT. The mode-locked titanium:sapphire laser was tuned to a wavelength $\lambda=800$ nm and had a duty cycle $\Delta \approx 10^{-5}$. Data are presented for three temperatures: 27 °C (triangles), 0 °C (squares), and -20 °C (circles). The error bars indicate the standard deviation for each data point. The three solid curves represent the best polynomial fits to the data sets [see Eq. (4)]. The dashed line of slope 2 represents quadratic behavior.

ode (Hamamatsu R464 PMT) is illustrated in Fig. 3 for incident light at a wavelength of 800 nm. The PMT was enclosed in a thermoelectric housing (Hamamatsu C4877) to adjust the temperature of the multialkali photocathode. The data are displayed as a double-logarithmic plot of the fundamental component of the photocurrent i (units of amperes) at the photocathode versus the mean optical power incident on the faceplate of the PMT (units of watts). The photocurrent at the anode was measured over a series of 3 min acquisition periods with the low-pass filter on the lock-in amplifier set to a bandwidth of 26 mHz. The current at the photocathode was calculated by dividing the measured anode photocurrent by the mean current gain $\bar{G} \approx 10^8$. The mean and standard deviations of the photocurrent were recorded at three temperatures: 27 °C (triangles), 0 °C (squares), and -20 °C (circles).

It is clear from the data displayed in Fig. 3 that the slopes of the curves increase toward a value of 2 as the incident optical power is augmented. This shows that the quadratic term in Eq. (4) increasingly dominates the linear term. For the -20 and 0 °C data, the slope ultimately reaches a value of 2 and the dominance is essentially complete. At 27 °C, however, the temperature is high enough that the Fermi-tail photocurrent is more robust (see Sec. IV) and the quadratic contribution fails to reach full dominance at the maximum optical power provided at the faceplate of the PMT. The two-photon photocurrent appears to be relatively insensitive to temperature for these semiconductor materials, as it is for metals.^{11,12}

The wavelength dependence of the two-photon photocurrent from the same K_2CsSb multialkali semiconductor is displayed in Fig. 4. The data were recorded at 27 °C for

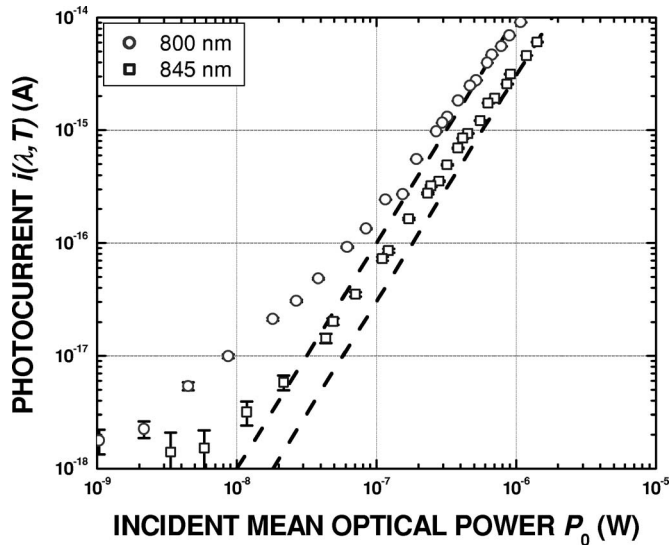


FIG. 4. Two-photon photoemission from a K_2CsSb -semiconductor photocathode in a Hamamatsu R464 PMT. The double-logarithmic plot displays the fundamental component of the photoelectric current at the cathode (amperes) vs the mean optical power (watts) incident on the faceplate of the PMT. The temperature of the PMT was fixed at 27°C . Data are presented for two wavelengths of the mode-locked titanium:sapphire laser: 800 nm (circles) and 845 nm (squares). The error bars indicate the standard deviation for each data point. The dashed lines of slope 2 indicate quadratic behavior.

wavelengths centered at $\lambda=800$ nm (circles) and at 845 nm (squares). Again, the slope increases toward a value of 2 as the optical power increases, indicating that the quadratic term increasingly dominates the linear term. At a given value of the optical power, the longer wavelength photons (845 nm $\Rightarrow h\nu=1.47$ eV) carry less energy per photon than the shorter wavelength photons (800 nm $\Rightarrow h\nu=1.55$ eV), but there are more of them. Because of its exponential dependence on energy, however, the Fermi tail plays a more dominant role for single-photon photoemission induced by the 800 nm photons and it therefore serves to increase the photocurrent.

IV. TEMPERATURE AND WAVELENGTH DEPENDENCE OF FERMI-TAIL PHOTOEMISSION

The Fermi-tail photocurrent can be unambiguously observed by removing the focusing lens in Fig. 2, whereupon the illumination area is increased to the size of the laser beam (≈ 3 mm). As is understood from Eq. (4), this suppresses the two-photon photoemission since its magnitude decreases dramatically as the illumination area is increased. To measure the temperature and wavelength dependences of the one-photon Fermi-tail photocurrent, we therefore used the experimental arrangement shown in Fig. 5. We carried out nearly identical sets of experiments to those reported in Sec. III.

The temperature dependence of the one-photon Fermi-tail photocurrent from a K_2CsSb multialkali semiconductor photocathode (Hamamatsu R464 PMT) is illustrated in Fig. 6 for incident light at a wavelength of 800 nm. The data are displayed as a double-logarithmic plot of the fundamental component of the photocurrent at the photocathode (am-

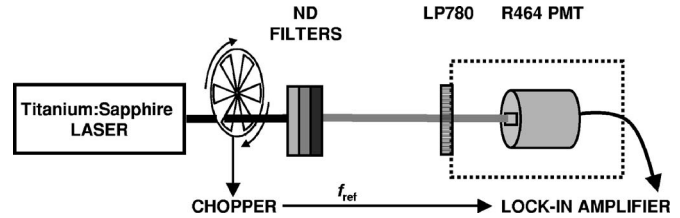


FIG. 5. Experimental arrangement for observing Fermi-tail (one-photon) photoemission. The arrangement is identical to that for two-photon photoemission, illustrated in Fig. 2, except that the lens is removed.

peres) versus the mean optical power P_0 (watts) incident on the faceplate of the PMT. The photocurrent at the anode of the PMT was measured over a series of 3 min acquisition periods with the low-pass filter on the lock-in amplifier set to a bandwidth of 26 mHz. The mean and standard deviations of the current were recorded at three temperatures: 27°C (triangles), 0°C (squares), and -20°C (circles). The current at the photocathode was determined by dividing the anode current by the mean current gain of the PMT, $\bar{G} \approx 10^8$.

The solid curves represent near-linear fits to each data set using the measured background current at each temperature. The associated one-photon Fermi-tail photoemission yields $Y_F(\lambda, T)$ are calculated by setting to zero the third term on the right-hand side of Eq. (4), which provides

$$Y_F(\lambda, T) = \frac{i(\lambda, T) - i_{\text{ckt}}}{\mathcal{F}_1(TP_0)}. \quad (13)$$

Values for the fixed experimental parameters are as follows: $i_{\text{ckt}} \approx 10^{-18}$ A, $\mathcal{F}_1 = 2/\pi$, and $T \approx 0.7$. For a particular data set, choosing a value of the observed photocurrent $i(\lambda, T)$, and its associated mean optical power P_0 , permits the Fermi-

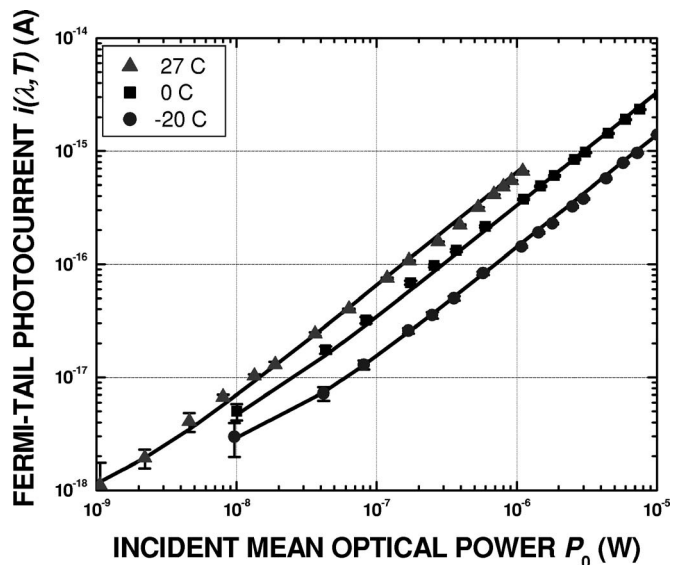


FIG. 6. Fermi-tail (one-photon) photoemission: double-logarithmic plot of the fundamental component of the photoelectric current at the cathode (amperes) vs the mean optical power (watts) incident on the faceplate of the R464 PMT, acquired at 27°C (triangles), 0°C (squares), and at -20°C (circles). The mode-locked titanium:sapphire laser was tuned to a wavelength $\lambda=800$ nm. The error bars indicate the standard deviation for each data point and the solid curves represent near-linear fits to each data set using the measured background current from the PMT.

TABLE I. Extracted experimental values of the one-photon Fermi-tail photoemission yield $Y_F(\lambda, T)$, and the two-photon photoemission yield $\Lambda(\lambda, T)$ (units are A/W in both cases), for several commercially available multialkali-semiconductor photocathode materials, for different values of the incident wavelength λ , and temperature T . The values for $Y_F(\lambda, T)$ and $\Lambda(\lambda, T)$ are obtained from Eqs. (13) and (14), respectively, and have therefore been corrected for additive circuit current, optical loss, the role of the mechanical light chopper, and the pulsed nature of the source. Values for the fixed experimental parameters are $i_{\text{ckt}} \approx 10^{-18}$ A, $\mathcal{F}_1 = 2/\pi$, $T \approx 0.7$, $\Gamma \approx 2 \times 10^5$, and $\mathcal{A} \approx 2.5 \times 10^{-5}$ cm². Mean values of the current gain for the R464, R2557, and 1P28 PMTs were $\bar{G} \approx 10^8$, 5×10^6 , and 10^7 , respectively. For the three materials the band gap energy and electron affinity are, respectively, 1 and 1.1 eV for K₂CsSb, (see Ref. 22) 1 and 1 eV for Na₂KSb, (see Ref. 10) and 1.6 and 0.4 eV Cs₃Sb (see Ref. 23). The intensity of the illuminated spot at the photosurface, \mathcal{I}_0 , is expressed in W/cm². The results are precise to within 10% but are accurate only to within a factor of 10 or so, owing principally to uncertainties in the optical losses, focused spot size, and mean current gain.

PMT MODEL NUMBER ^a	SEMICONDUCTOR	λ (nm)	T (K)	$Y_F(\lambda, T)$ (A/W)	$\Lambda(\lambda, T) = L(\lambda, T)\mathcal{I}_0$ (A/W)
R464	K ₂ CsSb	800	300	1.50×10^{-9}	$2.60 \times 10^{-12}\mathcal{I}_0$
			273	0.74×10^{-9}	$6.70 \times 10^{-12}\mathcal{I}_0$
		830	300	1.30×10^{-9}	$2.00 \times 10^{-12}\mathcal{I}_0$
			273	0.57×10^{-9}	$5.20 \times 10^{-12}\mathcal{I}_0$
		845	300	0.52×10^{-9}	$0.98 \times 10^{-12}\mathcal{I}_0$
			253	0.02×10^{-9}	$2.70 \times 10^{-12}\mathcal{I}_0$
R2557	Na ₂ KSb	800	300	5.30×10^{-7}	...
		845	300	0.68×10^{-7}	$7.10 \times 10^{-12}\mathcal{I}_0$
1P28	Cs ₃ Sb	800	300	6.00×10^{-8}	...
		845	300	0.62×10^{-8}	$0.18 \times 10^{-13}\mathcal{I}_0$

^aHamamatsu Photonics K.K.

tail photoemission yield $Y_F(\lambda, T)$ to be calculated.

Using this formula and these parameters, we have determined the one-photon Fermi-tail photoemission yields for multialkali-semiconductor photocathodes in three commercially available photomultiplier tubes at several temperatures and wavelengths: (1) K₂CsSb (potassium cesium antimonide) in the Hamamatsu R464, (2) Na₂KSb (sodium potassium antimonide) in the Hamamatsu R2557, and (3) Cs₃Sb (cesium antimonide) in the Hamamatsu 1P28. The results are provided in Table I. Generally speaking, for the range of parameters under consideration, we find that the one-photon Fermi-tail photoemission yield increases with increasing photocathode temperature and with decreasing wavelength of the illumination, in accordance with expectations.⁶ The value we obtain for Cs₃Sb, $Y_F(845 \text{ nm}, 300 \text{ K}) = 6.2 \times 10^{-9}$ A/W, is not far from that obtained by Imamura *et al.*,¹³ $Y_F(1060 \text{ nm}, 300 \text{ K}) \sim 10^{-9}$ A/W. The difference in reported values can be attributed to the longer incident wavelength used in the latter experiment.

If two-photon photoemission is the phenomenon of principal interest, it is usually desired to reduce the one-photon Fermi-tail photocurrent. It is clear from Fig. 6 that reducing the temperature of the PMT housing from 27 to 0 °C reduces the Fermi-tail photocurrent by a factor of ~ 2 . Reducing the temperature by an additional 20 °C again yields a similar reduction: a factor of ~ 2.3 . Over the temperature operating range of the cooled PMT housing, therefore, we can realize an overall reduction of about a factor of 4.6. It is expected that this contribution would continue to diminish with further cooling.

The wavelength dependence of the one-photon Fermi-tail photocurrent from the same K₂CsSb multialkali semicon-

ductor is displayed in Fig. 7. The data were recorded at 27 °C for wavelengths centered at $\lambda = 800$ nm (circles) and at 845 nm (squares). The associated one-photon Fermi-tail photoemission yields $Y_F(\lambda, T)$ are given in Table I. It is clear that the photocurrent can be reduced by an additional factor of ~ 2.7 by increasing the wavelength of the incident light from 800 to 845 nm.

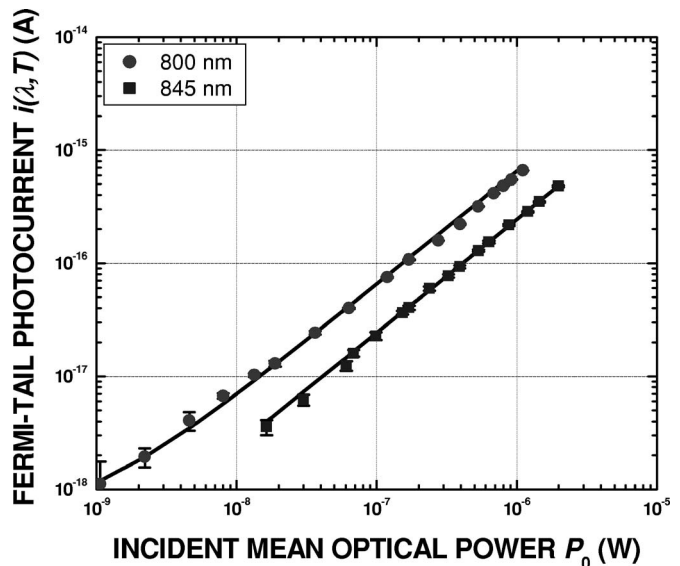


FIG. 7. Fermi-tail (one-photon) photoemission: double-logarithmic plot of the fundamental component of the photoelectric current (amperes) vs the mean optical power (watts) incident on the faceplate of the R464 PMT for $\lambda = 800$ nm (circles) and 845 nm (squares) at 27 °C. The error bars indicate the standard deviation for each data point and the solid curves represent near-linear fits to each data set, using the measured background current from the PMT.

Since the two-photon photocurrent in semiconductors is insensitive to temperature and relatively insensitive to wavelength over this range (as it is for metals), we conclude that the residual one-photon photocurrent arising from Fermi-tail electrons can be reduced by at least an order of magnitude by employing both detector cooling and longer wavelength sources.

V. TWO-PHOTON PHOTOEMISSION YIELD

The two-photon photoemission yield is calculated by making use of Eqs. (4)–(6), which provide

$$\Lambda(\lambda, T) = L(\lambda, T)(\mathcal{T}_0) = \frac{i(\lambda, T) - i_{\text{ckt}}}{\mathcal{F}_1(TP_0)\Gamma} - \frac{Y_F(\lambda, T)}{\Gamma}. \quad (14)$$

Values for the fixed experimental parameters are as follows: $i_{\text{ckt}} \approx 10^{-18}$ A, $\mathcal{F}_1 = 2/\pi$, $T \approx 0.7$, $\Gamma \approx 2 \times 10^5$, and $\mathcal{A} \approx 2.5 \times 10^{-5}$ cm². For a particular data set, choosing a value of the observed photocurrent $i(\lambda, T)$ and its associated mean optical power P_0 , along with the one-photon Fermi-tail photoemission yield $Y_F(\lambda, T)$ for that data set, permits the intensity of the light spot at the material, \mathcal{T}_0 , and thence the two-photon photoemission yield $\Lambda(\lambda, T)$ to be calculated.

Using these formulas and parameters, we determined the two-photon photoemission yields for multialkali-semiconductor photocathodes in three commercially available photomultiplier tubes at several temperatures and wavelengths: (1) K₂CsSb (potassium cesium antimonide) in the Hamamatsu R464, (2) Na₂KSb (sodium potassium antimonide) in the Hamamatsu R2557, and (3) Cs₃Sb (cesium antimonide) in the Hamamatsu 1P28.

Our findings are tabulated in Table I. The values are reasonably close to those reported earlier for similar materials;^{7,13} variations are expected given the uncertainties involved in the measurements. Generally speaking, for the range of parameters under consideration, we find that the two-photon photoemission yield is relatively insensitive to the temperature of the photocathode and wavelength of illumination.

Of the three PMT models we examined, we discovered that the R2557 PMT, with a sodium potassium antimonide photocathode, provides a two-photon photoemission yield that is slightly higher than the other models. However, a two-photon signal can be detected for this device at room temperature only if the Fermi-tail photocurrent is reduced by using wavelengths longer than 845 nm. And even at that wavelength, the two-photon photocurrent can only be observed across a narrow range of values of the incident mean optical power. This result stresses the importance of evaluating the magnitude of the Fermi-tail photocurrent which may ultimately reduce the contrast afforded by the semiconductor material for measuring two-photon processes.

For room temperature operation at shorter wavelengths, the R464, with a potassium cesium antimonide photocathode, is the best choice for observing two-photon photoemission since it has the lowest residual one-photon photocurrent of all three devices. For this PMT, it is possible to measure the two-photon photocurrent across at least an order of magnitude of the incident optical power under these conditions.

This range of incident power can be extended by cooling the device and/or increasing the wavelength of the incident light presented to the semiconductor photocathode.

For experiments with the R2557 and 1P28 PMTs carried out at wavelengths shorter than 845 nm, the residual one-photon photocurrent masked much of the two-photon photocurrent. Attempts to measure an appreciable two-photon photocurrent at incident powers greater than 20 μ W resulted in a saturation of the signal, possibly as a result of local heating of the photocathode. We therefore provide values for the two-photon photoemission yield only at a wavelength of 845 nm for these tubes. The small two-photon photoemission yield for the 1P28 PMT may result from the fact that the band gap energy exceeds the photon energy.

VI. CONCLUSION

Two-photon photoemission is a valuable technique for obtaining information about interface, surface, and image potential states in various materials; it also offers insights into the time evolution of the electron distribution following photon excitation.^{14–21} We have measured the temperature and wavelength dependences of two-photon photoemission from a number of multialkali-semiconductor materials that comprise the photocathodes of commercially available photomultiplier tubes. We identify those materials in which two-photon photoemission can be most readily observed. Two-photon photoemission exhibits a quadratic dependence on the incident optical power.

The observation of two-photon photoemission from multialkali semiconductors is facilitated by cooling the sample since the residual one-photon photocurrent arising from the Fermi tail is then reduced. The observation of two-photon photoemission is further facilitated by increasing the wavelength of the incident light, which serves to reduce access to electrons in the Fermi tail. We have therefore determined the temperature and wavelength dependences of one-photon Fermi-tail photoemission from these same multialkali-semiconductor materials. These measurements are essential for the proper design of experiments to observe entangled-photon photoemission, which, such as Fermi-tail photoemission, exhibits a linear dependence on the incident optical power.²²

ACKNOWLEDGMENTS

The authors acknowledge the assistance of Conor Maguire in collecting experimental data. This work was supported by the Center for Subsurface Sensing and Imaging Systems (CenSSIS), a National Science Foundation Engineering Research Center, by a U.S. Army Research Office (ARO) Multidisciplinary University Research Initiative (MURI) Grant, and by the David & Lucile Packard Foundation.

¹H. Y. Fan, *Phys. Rev.* **68**, 43 (1945).

²M. C. Teich, J. M. Schroeder, and G. J. Wolga, *Phys. Rev. Lett.* **13**, 611 (1964).

³H. Sonnenberg, H. Heffner, and W. Spicer, *Appl. Phys. Lett.* **5**, 95 (1964).

⁴P. Bloch, *J. Appl. Phys.* **35**, 2052 (1964).

⁵B. E. A. Saleh and M. C. Teich, *Fundamentals of Photonics* (Wiley, New York, 1991), Chap. 17.

⁶M. C. Teich and G. J. Wolga, *J. Opt. Soc. Am.* **57**, 542 (1967).

- ⁷M. C. Teich and G. J. Wolga, Phys. Rev. **171**, 809 (1968).
- ⁸M. C. Teich, Ph.D. thesis, Cornell University, 1966; <http://wwwlib.umi.com/dxweb/gateway>
- ⁹M. Göppert-Mayer, Ann. Phys. **9**, 273 (1931).
- ¹⁰C. Ghosh, Phys. Rev. B **22**, 1972 (1980).
- ¹¹R. H. Fowler, Phys. Rev. **38**, 45 (1931).
- ¹²L. A. DuBridge, Phys. Rev. **43**, 727 (1933).
- ¹³S. Imamura, F. Shiga, K. Kinoshita, and T. Suzuki, Phys. Rev. **166**, 322 (1968).
- ¹⁴S. Schuppler, N. Fischer, T. Fauster, and W. Steinmann, Phys. Rev. B **46**, 13539 (1992).
- ¹⁵W. S. Fann, R. Storz, H. W. K. Tom, and J. Bokor, Phys. Rev. B **46**, 13592 (1992).
- ¹⁶X. Y. Wang, R. Paiella, and R. M. Osgood, Jr., Phys. Rev. B **51**, 17035 (1995).
- ¹⁷T. Fauster, Surf. Sci. **507**, 256 (2002).
- ¹⁸C. Kentsch, M. Kutschera, M. Weinelt, T. Fauster, and M. Rohlfling, Phys. Rev. B **65**, 035323 (2002).
- ¹⁹L. Töben, T. Hannappel, R. Eichberger, K. Möller, L. Gundlach, R. Ernstorfer, and F. Willig, J. Cryst. Growth **248**, 206 (2003).
- ²⁰M. Lisowski, P. Loukakos, U. Bovensiepen, J. Stähler, C. Gahl, and M. Wolf, Appl. Phys. A: Mater. Sci. Process. **78**, 165 (2004).
- ²¹M. Weinelt, M. Kutschera, T. Fauster, and M. Rohlfling, Phys. Rev. Lett. **92**, 126801 (2004).
- ²²F. Lissandrin, B. E. A. Saleh, A. V. Sergienko, and M. C. Teich, Phys. Rev. B **69**, 165317 (2004).
- ²³T. Hattori, Y. Kawashima, M. Daikoku, H. Inouye, and H. Nakatsuka, Jpn. J. Appl. Phys., Part 1 **39**, 4793 (2000).